ACS OMEGA

http://pubs.acs.org/journal/acsodf

Article

Magnetic Nanoparticle-Based Surface-Assisted Laser Desorption/Ionization Mass Spectrometry for Cosmetics Detection in Contaminated Fingermarks: Magnetic Recovery and Surface Roughness

Sara A. Al-Sayed, Mohamed O. Amin, and Entesar Al-Hetlani*

Cite This: *ACS Omega* 2022, 7, 43894−43903

Read Online

ACCESS | Metrics & More | Article Recommendations | Supporting Information

ABSTRACT: In this work, we propose a matrix-free approach for the analysis of fingermarks (FMs) contaminated with five cosmetic products containing different active pharmaceutical ingredients (APIs) using surface-assisted laser desorption/ionization mass spectrometry (SALDI-MS). For this purpose, a magnetic SALDI substrate based on Fe_3O_4−CeO_2 magnetic nanoparticles was prepared, characterized, and optimized for the analysis of contaminated FMs without sample pretreatment. Initially, groomed FM and cosmetic products were separately analyzed, and their major components were successfully detected. Subsequently, FMs contaminated with Ordinary serum and Skinoren, Dermovate, Bepanthen, and Eucerin creams were analyzed, and components of FM and cosmetics were detected. The stability of the cosmetics in FMs was studied over an interval of 28 days, and all components showed good stability in FM for 4 weeks. Recovery of contaminated FMs from different surfaces utilizing a few microliters of the magnetic substrate was carried out using a simple external magnetic field from ceramic, plastic, metal, and glass. Successful retrieval of the API and FM components was achieved with magnetic recovery, and glass exhibited the best recovery, whereas ceramic tile demonstrated the lowest recovery. This was supported by atomic force microscopy study, which revealed that the ceramic surface had higher roughness than the other surfaces employed in this study, which adversely affected the magnetic maneuvering. This proof-of-concept investigation extends the application of SALDI-MS in forensic analysis of contaminated FMs by exploring cosmetics as exogenous materials and their stability and recovery from different surfaces.

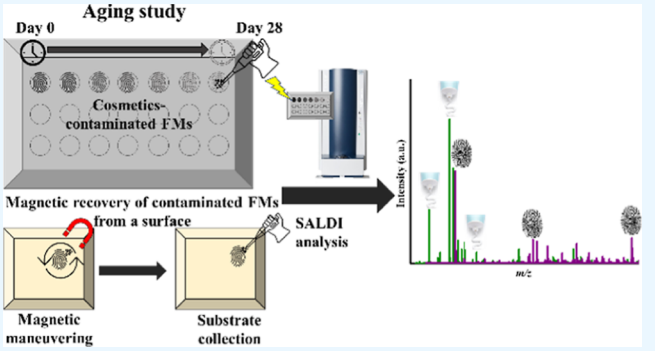

1. INTRODUCTION

Fingermarks (FMs) remain among the most important and powerful types of physical evidence in criminal investigations. The ridge impression of a FM carries physical and chemical components that can help reveal the identity of the donor or at least reveal some personal characteristics. Such findings are powerful in criminal investigations and can aid forensic investigators in their search for the identity of the perpetrator.[1] In particular, the chemical components of FMs have been the focus of several studies and have been comprehensively described by several researchers. The chemical components originate from body secretions (endogenous components) and contaminants (exogenous components). Specifically, exogenous component analysis has provided exceptionally valuable insights in criminal investigations by identifying the chemicals with which perpetrators came into contact before or while committing criminal acts.[2] In this regard, attenuated total reflection Fourier transform infrared (ATR−FTIR) spectroscopy has been utilized for the detection of ammonium nitrate, trinitrotoluene, and trinitrobenzene explosive particles in FMs,[3] whereas Raman spectroscopy has been used to analyze FMs contaminated with nonsteroidal anti-inflammatory drugs.[4] Chromatographic techniques such as ultrahigh-performance liquid chromatography coupled with mass spectrometry (MS) have been employed to obtain amino acid profiles from different donors.[5] Illicit drugs such as morphine, 6-acetyl morphine, and heroin in contaminated FMs have been detected using matrix-assisted laser desorption/ionization MS (MALDI-MS).[6] Further details on recent developments in the chemical analysis of FMs can be found in several review articles.[7−9]

Received: August 10, 2022
Accepted: November 9, 2022
Published: November 21, 2022

https://doi.org/10.1021/acsomega.2c05134
ACS Omega 2022, 7, 43894−43903

Cosmetics products are articles that are used to cleanse, beautify, enhance, and alter appearances. They can be categorized into different classes, including decorative products (makeup), skin care, hair care, soaps, and perfumes.[10] They are applied on the face, skin, or hair and can be transferred onto a variety of surfaces via day-to-day normal activities, such as using door handles, kitchenware, and furniture items.[11] Similar to FM evidence, the presence of cosmetic products indicates proof of physical contact. Over the last few years, cosmetic trace evidence has attracted much attention in the forensic community due to its ease of transfer and persistence on various types of surfaces.[12] It has been mainly linked to crimes of a sexual and violent nature, and some items, such as lipstick, can be used to send threatening notes and write suicide letters.[11] Recent research has focused on the analysis and differentiation of traces of different types of decorative products, such as nail polish,[13] lipstick,[14] foundation,[15] mascara,[16] and eyeliner.[17] For instance, Chophi et al.[18] utilized ATR−FTIR to discriminate among 73 nail polishes of the same shade. The same authors also used the aforementioned technique to discriminate fresh lipstick from different companies to study the effects of the wear time and the substrate onto which the lipstick was deposited.[19] Furthermore, Raman spectroscopy and partial least squares discriminant analysis were utilized for the analysis of 40 facial creams from eight brands.[20] However, creams, gels, and sera remain largely unexplored despite their common use by both sexes and various age groups. Additionally, the transfer of such evidence through touching and handling can produce FMs that are contaminated with externally applied products, thereby enriching the evidential value of the discovery.

Recent advances in surface science have led to the development of surface-assisted laser desorption/ionization MS (SALDI-MS), which has risen in popularity over the last few years in forensic analysis. In comparison to MALDI-MS, various nanostructured substrates have been engineered and have replaced conventional organic matrices to enable the detection of a wide range of small molecules, such as illicit drugs,[6] explosives,[21] poisons,[22] textile dyes,[23] and others.[24,25] SALDI-MS is a "dry" and "soft" ionization approach with minimum and predictable fragmentation patterns of the targeted analytes, which makes their identification easier.[26] We performed a successful preliminary study on the analysis of cosmetic creams, gels, and sera using SALDI-MS without sample pretreatment.[27] Herein, we expand upon the previous study by exploring the analysis of cosmetic product traces in FMs using magnetic nanoparticles (MNPs) as SALDI substrates. CeO_2 NPs displayed a strong absorbance over the visible and UV regions, a large surface area, and a small size;[24,25] therefore, we believe that incorporation of CeO_2 onto the MNPs can enhance (1) absorption of the laser irradiation, (2) transfer of the absorbed energy to the analyte, and (3) ionization efficiency of the analytes. Thus, FMs contaminated with Ordinary serum and Skinoren, Dermovate, Bepanthen, and Eucerin creams are analyzed, and components corresponding to the FMs and ingredients in the five products are successfully detected. Aging on a target plate and magnetic recovery of the contaminated FMs from four hard non-absorbing surfaces are performed utilizing Fe_3O_4−CeO_2 MNPs.

2. EXPERIMENTAL SECTION

2.1. Chemicals and Reagents. Ferric chloride ($FeCl_3$), ferrous chloride ($FeCl_2$), cerium(III) nitrate hexahydrate ($Ce(NO_3)_3{\cdot}6H_2O$), ammonium hydroxide, nicotinamide ≥99.5%, and ethanol were purchased from Sigma-Aldrich. All chemicals were used without further purification. Double-distilled water was obtained from an Elix Milli-Q water deionizer and used in all experiments.

Five cosmetic products were purchased from local pharmacies: Ordinary niacinamide 10% + zinc 1% serum (10% nicotinamide), Bepanthen cream (5% dexpanthenol), Dermovate cream (0.05% clobetasol propionate), Eucerin UreaRepair (10% urea), and Skinoren (20% azelaic acid). The composition of each product according to the corresponding leaflet and the chemical structures of the active pharmaceutical ingredients (APIs) are presented in Table S1.

2.2. Synthesis of Fe_3O_4−CeO_2 MNPs. Fe_3O_4−CeO_2 MNPs were prepared using five mass ratios of Fe_3O_4/CeO_2 (1:6, 1:9, 1:12, 1:15, and 1:18) according to the method published in ref 28 with some modifications. Fe_3O_4 MNPs were synthesized, and their surfaces were decorated with CeO_2 NPs. First, 6.00 g of $FeCl_3$ and 1.875 g of $FeCl_2$ were dissolved in 100 mL of deionized water and vigorously stirred under a N_2 atmosphere for 30 min at room temperature. Then, 15 mL of NH_4OH solution was added dropwise to the mixture, which resulted in the instantaneous formation of a black precipitate, and the reaction mixture was allowed to mix for 30 min. The resulting precipitate was collected, washed several times with distilled water and ethanol, and then dried overnight at 80 °C. For the fabrication of Fe_3O_4−CeO_2 MNPs, different amounts of $Ce(NO_3)_3{\cdot}6H_2O$ (1.2, 1.8, 2.4, 3, and 3.6 g for the ratios 1:6, 1:9, 1:12, 1:15, and 1:18, respectively) were dissolved in 100 mL of DI water, and Fe_3O_4 NPs were added to the solution under stirring. Subsequently, NH_4OH solution was introduced dropwise until the pH reached 9.7, and the reaction was allowed to proceed for 15 min. Finally, the resultant precipitate was centrifuged, washed with distilled water and ethanol, and dried overnight at 80 °C.

2.3. Characterization of Fe_3O_4−CeO_2 MNPs. Surface elemental analysis of the Fe_3O_4−CeO_2 MNPs was carried out by X-ray photoelectron spectroscopy (XPS), and the binding energies were referenced to the C 1s peak at 284.60 eV. X-ray diffraction (XRD) patterns were obtained using a Bruker D8 advanced diffractometer with a Cu Kα radiation source (λ 1/4 0.1542 nm). UV−vis spectroscopy was employed to study the optical properties of the obtained material using an Agilent Cary 5000 Scan UV−vis−near-infrared (UV−vis−NIR) spectrophotometer. To measure the surface area of the prepared material, the Brunauer−Emmett−Teller (BET) method was used, and nitrogen sorption isotherms of the sample were obtained at −195 °C using a Micromeritics Gemini VII ASAP 2020 automatic sorptometer (USA). Magnetic measurements were performed using a Mini cryogen-free 5 T system (Cryogenics Ltd. London, UK). The magnetization of the sample was measured using a vibrating-sample magnetometer (VSM) at room temperature (295 K) with a sensitivity of 10−6 emu and a maximum magnetic field strength of 5 T. The morphology and particle size of the MNPs were captured using an XF-416 camera (TVIPS, Germany). Samples were dispersed in ethanol and dropped onto a carbon support film. The roughness of the surfaces was investigated via atomic force microscopy (AFM)

https://doi.org/10.1021/acsomega.2c05134
ACS Omega 2022, 7, 43894−43903

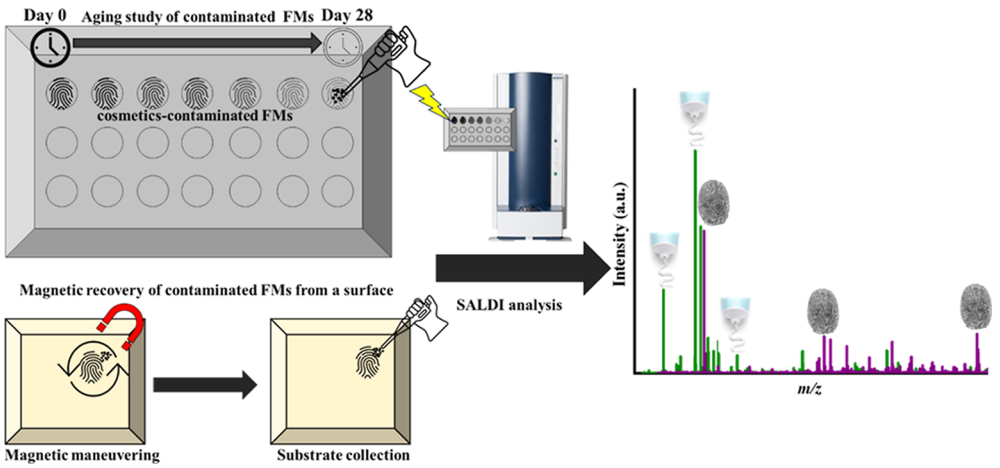

Figure 1. Illustration of the proposed methodology and approach for the analysis of cosmetics contaminated FMs.

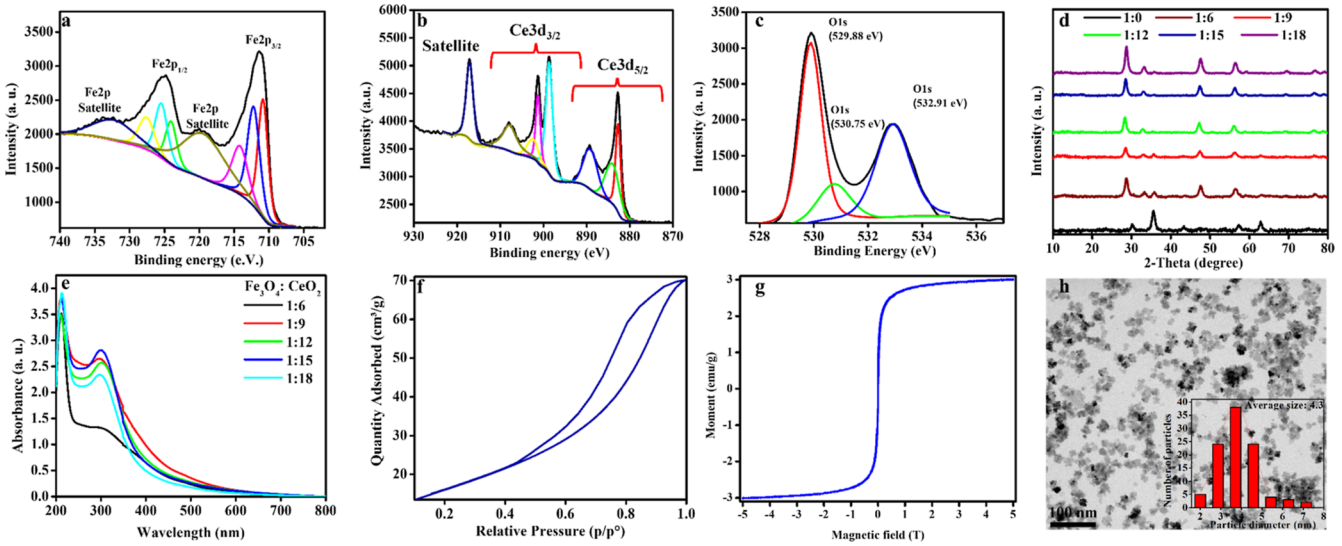

Figure 2. Characterization of Fe_3O_4−CeO_2 MNP XPS spectra of (a) Fe, (b) Ce, and (c) O; (d) XRD patterns of Fe_3O_4, CeO_2, and Fe_3O_4−CeO_2 MNPs; (e) UV−vis spectra for different ratios of CeO_2 on Fe_3O_4 MNPs; (f) BET isotherm; (g) VSM hysteresis loop for Fe_3O_4−CeO_2 MNPs with a ratio of 1:15; and (h) TEM image of Fe_3O_4−CeO_2 with a ratio of 1:15 (the inset shows the particle size distribution).

with a Nanoscope IV Multimode atomic force scanning probe microscope using a model VEECO-Nanoscope IV multiple AFM/SPM.

2.4. Fingermark (FM) and Cosmetic Product Preparation. Initially, FM and cosmetic product smudges were analyzed separately as control samples using SALDI-MS; subsequently, FMs contaminated with the traces of each cosmetic product were studied. Gloves were used in these experiments to avoid cross contamination. The FM impressions were collected from a single female donor. The donor washed her hands thoroughly with soap and water and, after drying, rubbed her index finger over her forehead a couple of times to stimulate sebaceous glands and then placed the index finger directly on the target plate; the resulting FM is referred to as a groomed FM. Additionally, 5 mg of each product was weighed and smeared over the target plate and allowed to dry at room temperature. Similarly, FMs contaminated with cosmetic products were prepared by following the same procedure with an additional step of evenly rubbing a small amount of one of the cosmetic products on the donor's index finger before the FM was deposited on the target plate and left to dry at room temperature prior to analysis.

The effects of aging on the FMs contaminated with cosmetics that were deposited on the target plate were analyzed throughout an interval of 28 days. Spectra were obtained at 0, 1, 2, 3, 7, 14, 21, and 28 days after FM deposition.

2.5. Magnetic Recovery of Contaminated FMs from Different Surfaces. The prepared MNPs were employed for the magnetic recovery of FMs contaminated with cosmetic products from four different surfaces by magnetic forces. The effect of the surface on the detection of APIs was mainly explored. Initially, cosmetics-contaminated FMs were deposited on four surfaces: aluminum (nonmagnetic metal), ceramic, glass, and plastic. Next, 25 μL of Fe_3O_4−CeO_2 MNP solution (2 mg/mL) was applied to the contaminated FMs and maneuvered across each surface using a magnet for approximately 10 s, as demonstrated by Amin et al.[29] The same steps were repeated to enable the maximum recovery of the cosmetic product and FM components. Finally, the substrate was collected using a pipette and deposited on the

https://doi.org/10.1021/acsomega.2c05134
ACS Omega 2022, 7, 43894−43903

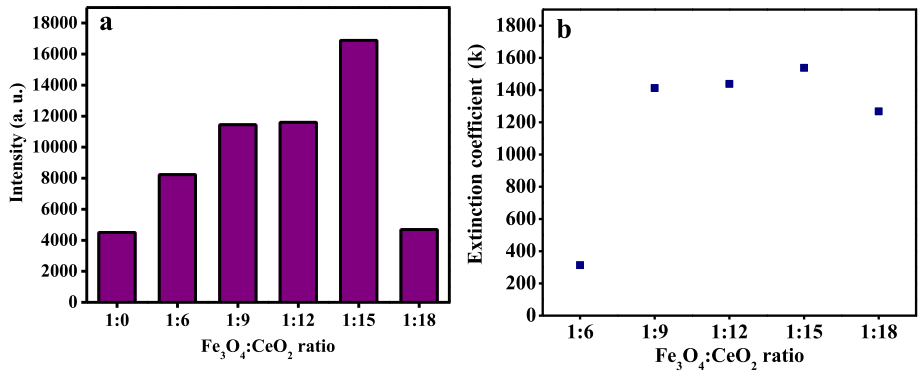

Figure 3. (a) Signal intensities in the SALDI-MS analysis of nicotinamide standard solution using different CeO_2 ratios and (b) extinction coefficient values calculated at different Fe_3O_4/CeO_2 ratios.

target plate for analysis. Figure 1 illustrates the proposed methodology and approach for the analysis of cosmetics contaminated FMs.

2.6. SALDI-MS Analysis of FMs. SALDI-MS analysis was performed using a Bruker ultrafleXtreme MALDI-TOF/TOF-MS system equipped with a Smartbeam-II. The analysis of the nicotinamide standard solution, FMs, cosmetics, and FMs contaminated with cosmetic products was performed in positive ionization mode, and the spectra were acquired using a random walk raster with a frequency of 2000 Hz over a mass range of 40−1500 Da, an ion source voltage of 25.0 kV, and a reflector voltage of 26.6 kV. The instrument was calibrated prior to the analyses using a ProteoMass Calibrant (Sigma-Aldrich, Chemie GmbH, Schnelldorf, Germany) mixed within the normal range, and the data were processed using Bruker flexAnalysis (Bruker, Germany).

The reproducibility of the analyses was determined by obtaining 10 spectra for each sample and computing the average analyte signal intensities and relative standard deviations (% RSDs).

3. RESULTS AND DISCUSSION

3.1. Characterization of the Fe_3O_4−CeO_2 MNPs. Initially, the surface elemental composition and oxidation states of Fe, Ce, and O of the Fe_3O_4−CeO_2 MNPs were investigated via XPS. Figure 2a−c presents the XPS spectra of Fe, Ce, and O. In Figure 2a, the binding energies (BEs) at 710.8 and 724.0 eV correspond to Fe $2p_{3/2}$ and Fe $2p_{1/2}$, respectively, which are characteristic of Fe_3O_4.[30] The two main peaks were deconvolved into six peaks at 712.2 and 714.2 eV, which correspond to Fe $2p_{3/2}$; 725.4 and 727.6 eV, which are assigned to Fe $2p_{1/2}$; and two satellite peaks at 719.4 and 732.3 eV. Additionally, the BEs at 882.7, 889.1, and 898.7 eV can be ascribed to Ce $3d_{5/2}$, and those at 901.3, 907.8, and 917.0 eV are assigned to Ce $3d_{3/2}$, which corresponds to the Ce^{4+} state,[31] whereas the BEs at 884.1 and 902.4 eV, which correspond to Ce $3d_{5/2}$ and Ce $3d_{3/2}$, respectively, are attributed to the valence state of Ce^{3+},[32] as shown in Figure 2b. Finally, the O 1s spectrum in Figure 2c was deconvolved into three peaks: 529.9 eV, which can be ascribed to O^{2-},[33] and 530.7 and 532.9 eV, which are related to loosely bound oxygen, hydroxyl groups, or water adsorbed in the vacant sites of the lattice and on the surface.[32]

Figure 2d shows the XRD patterns of the synthesized Fe_3O_4−CeO_2 samples and pristine Fe_3O_4 NPs. The diffraction peaks for CeO_2 at 2θ = 28.5, 33.0, 47.4, 56.3, 59.0, 69.4, 76.7, and 79.0° are indexed to the (111), (200), (220), (311), (222), (400), (331), and (420) reflection planes, respectively. The characteristic diffraction peaks of CeO_2 NPs with face-centered cubic lattice structures are consistent with the corresponding Joint Committee on Powder Diffraction Standards data [JCPDS card (04-0593)].[34] The Fe_3O_4 diffraction peaks at 2θ = 30.2, 35.5, 43.2, 57.1, and 62.7° correspond to the lattice planes (220), (311), (400), (511), and (440), respectively, which is consistent with the corresponding JCPDS card (01-088-0315), which indicates the formation of the face-centered cubic lattice structure of Fe_3O_4.[35] XRD patterns of the synthesized Fe_3O_4−CeO_2 MNPs (Figure 2d) show a diffraction peak of Fe_3O_4 at 2θ = 35.5° for Fe_3O_4−CeO_2 ratios of 1:6 and 1:9, which disappears at higher CeO_2 concentrations; this could be due to the presence of a high loading of CeO_2 NPs in comparison to Fe_3O_4 NPs.

Strong UV absorbance of SALDI-MS substrates generally enhances the ionization and desorption of the analyte;[36] therefore, the prepared Fe_3O_4−CeO_2 MNPs were further characterized via UV−vis spectroscopy to investigate their optical properties. The initial assessment involved the analysis of pristine Fe_3O_4 and CeO_2 NPs, as demonstrated in Figure S1. CeO_2 NP absorption bands were observed in the visible and UV regions at 207 and 303 nm, respectively, with a maximum absorption at λ_{max} = 303 nm for Ce^{4+} in CeO_2,[37] and continuous absorption in the visible range is one of the characteristic features of iron oxide NPs.[38] The UV absorption spectra of Fe_3O_4−CeO_2 MNPs at different CeO_2 ratios, as presented in Figure 2e, exhibited strong absorbance over the visible and UV regions, which indicates a mixed behavior of both Fe_3O_4 and CeO_2 NPs. Furthermore, as the amount of CeO_2 that was added to Fe_3O_4 increased, the maximum absorption of the magnetic substrate increased at λ_{max} = 303 nm, reaching a maximum at a 1:15 ratio, and then the absorbance signal slightly decreased.

The size and porosity of the SALDI substrate play major roles in the desorption/ionization efficiency and detection;[39] thus, the surface area, pore size, and pore volume were determined for the fabricated substrate using N_2 adsorption−desorption, and the results are summarized in Table S2. Figure 2f presents the adsorption isotherms for all prepared substrates, which indicate that each prepared material exhibited a type IVa isotherm and H1 hysteresis loop, suggesting the presence of uniform mesopores in Fe_3O_4−CeO_2 MNPs.[40] A small decrease in the surface area was observed as the ratio of CeO_2 increased, indicating that the surface area was not drastically influenced. The magnetic properties of the prepared Fe_3O_4−CeO_2 substrate were studied

https://doi.org/10.1021/acsomega.2c05134
ACS Omega 2022, 7, 43894−43903

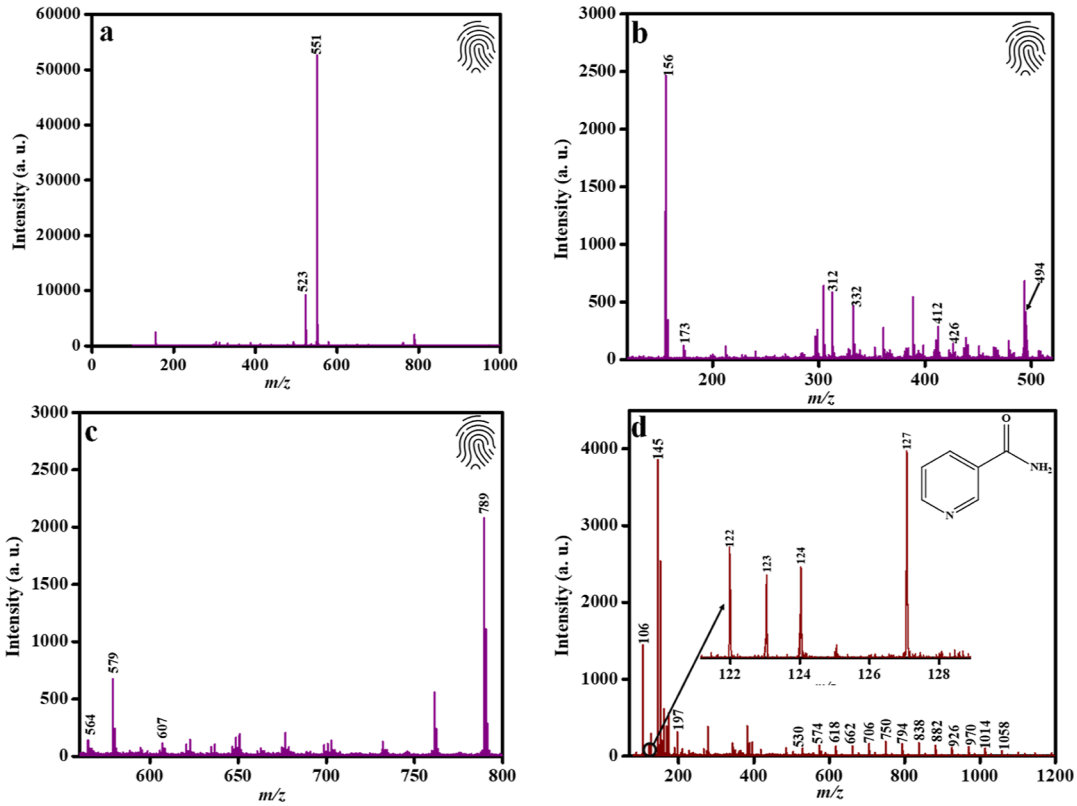

Figure 4. SALDI-MS analysis of control FM and Ordinary serum (as representative cosmetic products) samples obtained using Fe_3O_4−CeO_2 MNPs: (a) spectrum of the groomed FM, (b) enlargement of **a** from m/z 100−500, (c) enlargement of **a** from m/z 550−800, and (d) the Ordinary serum spectrum m/z between 100 and 1400. The inset shows m/z 529−1058, which corresponds to poly(ethylene oxide).

via VSM at 295 K, as shown in Figure 2g. The magnetic hysteresis loop demonstrated the superparamagnetic behavior (zero coercivity value) of the prepared substrate, with a saturation magnetization (M_s) of 3.02 emu/g.[28]

Finally, the morphology and average particle size of the synthesized MNPs were determined using transmission electron microscopy (TEM), as illustrated in Figure 2h. The prepared MNPs were hemisphere-shaped, and their average particle size was approximately 4.3 nm (inset in Figure 2h). Since particles of small size provide good desorption/ionization, these findings imply that Fe_3O_4−CeO_2 MNPs can be a good candidate for SALDI analysis.

3.2. Effect of the Loading Amount of CeO_2 NPs on the SALDI Performance. In this work, CeO_2 NPs at various ratios on a magnetic substrate were prepared, and their effect on the performance of SALDI-MS was investigated to identify the optimum composition of the prepared substrate. Therefore, a standard solution of nicotinamide, which is an API in one of the cosmetics used in this study, namely, niacinamide 10% + zinc 1% serum, was employed as the model analyte, and its SALDI signal intensity was measured using 1:6, 1:9, 1:12, 1:15, and 1:18 Fe_3O_4−CeO_2 MNPs. As illustrated in Figure 3a, the signal intensity of the detected analyte increased gradually upon the addition of CeO_2 NPs and stabilized at ratios of 1:9 and 1:12, and the highest signal intensity was recorded at 1:15 ratio, which then declined at 1:18 Fe_3O_4−CeO_2 MNPs. The optimum SALDI-MS signal that was obtained is consistent with the UV−vis absorbance (Figure 2e), where a 1:15 ratio of Fe_3O_4−CeO_2 showed the highest absorption of the well-defined peak at 303 nm compared to other ratios of the Fe_3O_4−CeO_2 magnetic substrate. In SALDI-MS, laser photons are absorbed by the substrate prior to their transfer to the analyte to promote the ionization and desorption of the analyte. Large surface area, good UV absorption, and low thermal conductivity are considered driving factors in ionization and desorption processes. A large surface area is desirable for the adsorption and retention of the analyte molecules, and it also contributes to laser beam refraction.[41] Furthermore, a large extinction coefficient (k) in the UV region is required for efficient absorption of the laser beam by the substrate;[42] thus, the UV extinction coefficients of the prepared substrates were calculated using the equations below and are displayed as functions of the Fe_3O_4/CeO_2 ratio in Figure 3b.

$$\alpha = \frac{2.303 \times A}{d} \quad (1)$$

$$k = \frac{\alpha\lambda}{4\pi} \quad (2)$$

where α is the absorption coefficient (a.u.), A is the absorbance (a.u.), d is the sample thickness (cm), and λ is the wavelength (nm).[43,44]

The highest extinction coefficient was obtained using 1:15 Fe_3O_4−CeO_2, which reflects how strongly the substrate absorbs radiation at a specific wavelength.[42]

3.3. SALDI-MS Analysis of FM and Cosmetic Products Using Fe_3O_4−CeO_2 MNPs. FM comprises a complex mixture of endogenous organic (such as amino acids, proteins, fatty acids, wax esters, cholesterol, vitamins, and enzymes) and inorganic ions (Na, Ca, K, and Cl) that are secreted by eccrine glands and sebaceous glands with a minor contribution from

https://doi.org/10.1021/acsomega.2c05134
ACS Omega 2022, 7, 43894−43903

apocrine sweat. Other constituents of skin surface residues, such as carboxylic acids and short-chain alcohols, can also be found in FMs.[8,45] Furthermore, a countless number of materials from external sources can end up on the fingertips from daily tasks; these include pharmaceuticals, food stuff, and cosmetics, among others. Thus, in this study, FMs contaminated with cosmetic products were investigated using SALDI-MS to analyze their potential to provide forensically relevant information. Initially, FM and cosmetic product smudges were analyzed separately as control samples using SALDI-MS and the optimized Fe_3O_4−CeO_2 MNPs. First, mass spectra were obtained for the groomed FMs and the Ordinary serum (Figure 4a−d) and Skinoren, Dermovate, Bepanthen, and Eucerin creams (Figure S2a−d). The obtained ions and their corresponding m/z, average intensity, and % RSD values for the cosmetic products are presented in Tables S3 and S4. Through the chemical analysis of FMs, several endogenous components were detected, such as amino acids, fatty acids (FAs), diglycerides, triglycerol, squalene, and protonated and potassiated ions of cholesterol, as shown in Figure 4a−c; these substances were previously reported in FMs in several articles.[46−48] Additionally, a prominent contribution of dimethyldioctadecylammonium ions was observed in the spectrum of the FM at m/z 494.56, 522.59, and 550.63, which have been previously detected as exogenous contaminants of FMs (Figure 4a).[49]Figure 4d presents the positive ion mass spectrum of the Ordinary serum in which APIs were clearly observed in various forms, namely, $[niacinamide]^{\bullet+}$, $[niacinamide + H]^+$, $[niacinamide + 2H]^+$, $[niacinamide + Na]^+$, and $[niacinamide + K]^+$ at m/z 122.01, 123.04, 124.04, 145.06, and 161.05, respectively. Furthermore, additional ingredients were also detected in different forms, including pentylene glycol and dimethyl isosorbide (Table S4). Interestingly, the molecular mass distribution of polyethylene oxide was observed over a range of m/z 529−1058 with a repeating unit of 44.03 Da, which corresponds to the ethylene oxide monomer.[50] Other spectra of the cosmetics are shown in the Supporting Information, and the detected ingredients are summarized in Table S4. Figure S2a shows the mass spectrum of Skinoren cream, which confirmed the successful detection of the API azelaic acid in sodiated and potassiated adducts at m/z 211.09 and 227.06, respectively. Additional peaks were also observed at m/z 311.29 and 381.29, which can be assigned to hexadecyl 2-ethylhexanoate and glycerol monostearate, respectively. The positive-ion mass spectrum of Dermovate cream (Figure S2b) showed peaks for the API clobetasol propionate at m/z 466.19 and 468.20, which correspond to radical and deprotonated ions of the API. Moreover, excipients present in the cream were also detected, including stearyl alcohol, glyceryl monostearate, and cetosteryl alcohol. The mass spectrum of Bepanthen cream confirmed the detection of dexpanthenol (API) in three forms, namely, protonated, sodiated, and potassiated ions at m/z 206.13, 228.12, and 244.09, respectively, as depicted in Figure S2c. Finally, the spectrum of Eucerin cream, which is displayed in Figure S2d, shows peaks at m/z 83.02, 98.99, 115.03, 128.01, and 131.01, which correspond to the APIs and other ingredients in the cream and were assigned to $[urea + Na]^+$, $[urea + K]^+$, $[glycerin + Na]^+$, $[glycerin + K]^+$, and $[alanine + K]^+$, respectively. More importantly, a peak at m/z 143.09 was observed, which can be attributed to the fragment of carnitine $[carnitine\text{-}H_2O]^+$; carnitine was previously detected using mass spectrometry.[51]

3.4. SALDI-MS Analysis and Aging Study of FMs Contaminated with Cosmetic Products. FM physical features can be used to identify an individual by comparing the ridge characteristics between a FM from the crime scene and a FM from the perpetrator. However, if the features are not clear enough for physical comparison, chemical analysis can be conducted to identify characteristics of the donor. This can provide further information in cases related to sexual and violent assaults. Few studies have been conducted using SALDI-MS for the chemical analysis of exogenous components of FMs, such as drugs of abuse, pharmaceutical drugs, and explosives, as illustrated in Table S5. Different techniques used in the analysis of cosmetics, instruments employed, sensitivity, cost and time, cosmetics products analyzed, and limitations are provided in Table S6. In this regard, SALDI-MS was employed in the analysis of cosmetics-contaminated FMs. Ordinary serum and Skinoren, Dermovate, Bepanthen, and Eucerin creams were used to produce contaminated FMs, which were then deposited on a target plate and subjected to SALDI-MS analysis. Figure 5a (bottom spectrum) shows the representative mass spectrum of a fresh FM contaminated with Ordinary niacinamide serum, which confirmed the successful detection of endogenous components of the FM, including histidine, threonine, squalene, cholesterol, and FA (20:1), in addition to exogenous components from the serum, such as niacinamide, pentylene glycol, and dimethyl isosorbide. Similarly, both endogenous components of the FMs and exogenous substances from the cream/serum (as described in Section

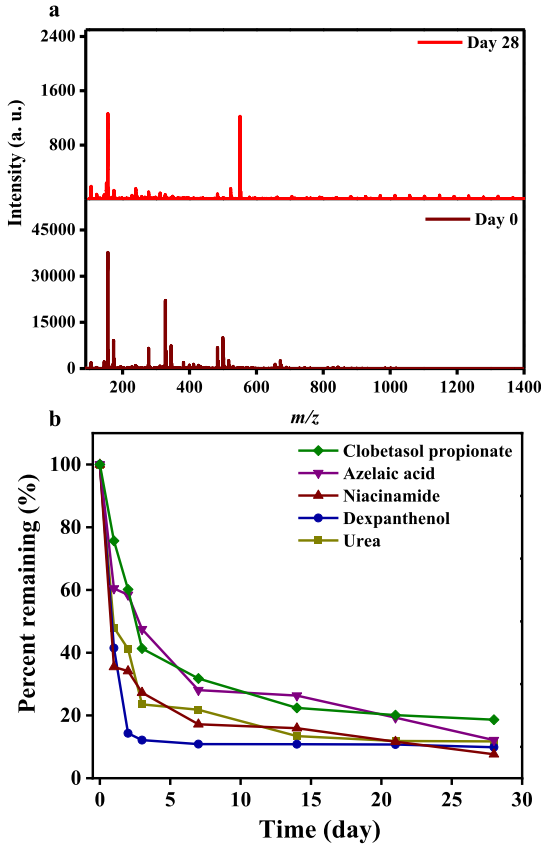

Figure 5. (a) SALDI-MS spectra of fresh and 28 day-old FMs that are contaminated with Ordinary serum. (b) Effect of aging on cosmetic product-contaminated FMs over 28 days expressed as the percent remaining of the APIs of each cosmetic product.

https://doi.org/10.1021/acsomega.2c05134
ACS Omega 2022, 7, 43894−43903

3.3) were observed in the mass spectra of all FMs that were contaminated by cosmetic products, as depicted in Figure S3a−d. These findings suggest that the direct detection of several endogenous and exogenous components of FMs is possible without sample pretreatment.

As an additional form of FM analysis, the time since deposition (TSD) can be assessed, which can help investigators estimate when a crime occurred and determine if a FM is relevant to the crime being investigated. However, evaluating the TSDs of FMs in crime scenes is challenging due to the influence of several variables, such as environmental conditions and the presence of exogenous substances, which can affect the kinetic degradation of the FMs. Thus, as a preliminary study, we investigated the effect of time on the stability of the APIs in contaminated FMs. For this purpose, an aging study was carried out under ambient conditions, where FMs contaminated with Ordinary serum (Figure 5a) and Skinoren, Dermovate, Bepanthen, and Eucerin creams (Figure S4a−d) were exposed to light, room temperature, and humidity, and the percent remaining over an interval of 28 days for each API was calculated, as shown in Figure 5b. Although the APIs exhibited various degrees of degradation, their detection was successful even 28 days after deposition. For the Ordinary serum, the remaining percentage of nicotinamide significantly dropped to less than 40% after 1 day of deposition, then gradually decreased with time, and finally reached 7.6% after 28 days. Moreover, for Bepanthen cream, dexpanthenol showed limited stability, where the percent remaining was 41% after 1 day, which decreased sharply from the second day and stabilized at approximately 10% of the original signal. Furthermore, clobetasol propionate in Dermovate exhibited good stability over time, where the percent remaining slowly decreased throughout the first 3 days and then plateaued at approximately 20% after 28 days. In contrast, Eucerin cream, which contains urea as the API, showed a large drop of 50% after 1 day and then stabilized after 14 days. Finally, the azelaic acid signal declined to 50% after 3 days and eventually reached 12% of the original signal. These findings prove the ability to detect traces of FMs contaminated with cosmetic products even 28 days after deposition with exposure to environmental conditions, which reflects the potential of SALDI-MS for investigating the stability of exogenous materials in FMs. Nevertheless, in the future, we believe that further analyses should be performed for longer periods of time and that more variables that might affect the kinetics of exogenous and endogenous materials in FMs should be evaluated. These variables include the races and ages of the donors and environmental parameters such as temperature, humidity, and exposure to light.

3.5. Magnetic Recovery of FMs Contaminated with Cosmetic Products from Different Surfaces. FMs can be deposited on a variety of surfaces due to normal daily activities; they can be in the form of complete or partial prints, empty areas, or just marks. The collection of FMs from different surfaces for analysis can be challenging; currently, the use of adhesive tapes is the most popular way to recover FMs; yet in some cases, they can interfere with the analysis.[52] Thus, we propose the magnetic recovery of FMs contaminated with cosmetic products as a simple approach for obtaining information from FMs on surfaces that are immobile or not convenient for instrumental analysis. Four nonporous hard surfaces, namely, ceramic tile, aluminum (nonmagnetic metal), glass, and plastic, were investigated by depositing FMs contaminated with Ordinary serum and Skinoren, Dermovate, Bepanthen, and Eucerin creams. The unique feature of this approach is the dual functionality of the MNPs: in addition to being the source of actuation, they provide a solid support for analyte adsorption.[53] The magnetic recovery of the FMs contaminated with cosmetic products was carried out, as described in Section 2.5. The FM components that were recovered from all surfaces showed m/z peaks corresponding to histidine, threonine, squalene, and cholesterol. The mass spectra of FMs contaminated with Ordinary serum that were recovered from ceramic, plastic, metal, and glass are shown in Figure 6a, while FMs that were contaminated with other creams are shown in Figures S5−S9. The SALDI-MS signal intensity of each API in the contaminated FMs that were recovered from the aforementioned surfaces is shown in Figure 6b.

Interestingly, the ceramic tile exhibited the lowest recovery signal for the majority of the cosmetic products, while glass produced good results for most of the products. Overall, it was observed that Dermovate cream (clobetasol propionate) was the hardest to recover using magnetic forces on all surfaces, whereas Bepanthen (dexapenthanol) and Eucerin (urea) exhibited good recovery.

The clobetasol propionate signal was stable for plastic and metal and slightly decreased for both glass and ceramic tile. The azelaic acid recovery was the highest from glass, followed by plastic and metal, and the lowest signal was recorded for the ceramic tile, which could be due to the highly hydrophobic nature of the cream and its limited miscibility with the MNP suspension used for recovery (similar behavior was obtained using methanol and acetonitrile). The recovery of niacinamide from the Ordinary serum followed a similar trend as that of clobetasol propionate. The detected signal was high from both the glass and metal surfaces and was lowest from the plastic and ceramic surfaces. The Ordinary serum-contaminated FMs dispersed immediately after the addition of the substrate on the plastic and ceramic surfaces and were slightly difficult to recover. The signal drastically decreased for the Skinoren (azelaic acid) and Dermovate (clobetasol propionate) creams from ceramic, which could have been due to the high roughness of the ceramic surface. Finally, the recovery signals of the aqua-rich moisturizers Bepanthen (dexpanthenol) and Eucerin (urea) were the highest from glass, followed by metal, ceramic, and plastic.

The obtained recovery results exhibited great variations among the products and types of surfaces that were used. Movements of droplets of a liquid that contains MNP substrate for recovery over FM-contaminated impressions deposited on a surface are influenced by several factors, such as the roughness of the surface, the friction between the MNPs and the surface, the adhesion of the MNPs to the surface, the surface tension, and the applied magnetic forces.[53] In this respect, we investigated the surface roughness, as the surfaces vary in terms of smoothness and adhesion can result from the sticky nature of the cosmetics and the presence of polymers and waxes. AFM was employed to obtain information about the roughness of the surfaces employed in this study to evaluate the recovery behavior of the cosmetics in FMs. The 3D topographies (3 μm × 3 μm) of the surfaces are presented in Figure 6c−f, and the average roughness (R_a) for each surface was determined as the average roughness among all points along the length of the line investigated in the middle of the obtained AFM images. A mountain-like morphology with deep

https://doi.org/10.1021/acsomega.2c05134
ACS Omega 2022, 7, 43894−43903

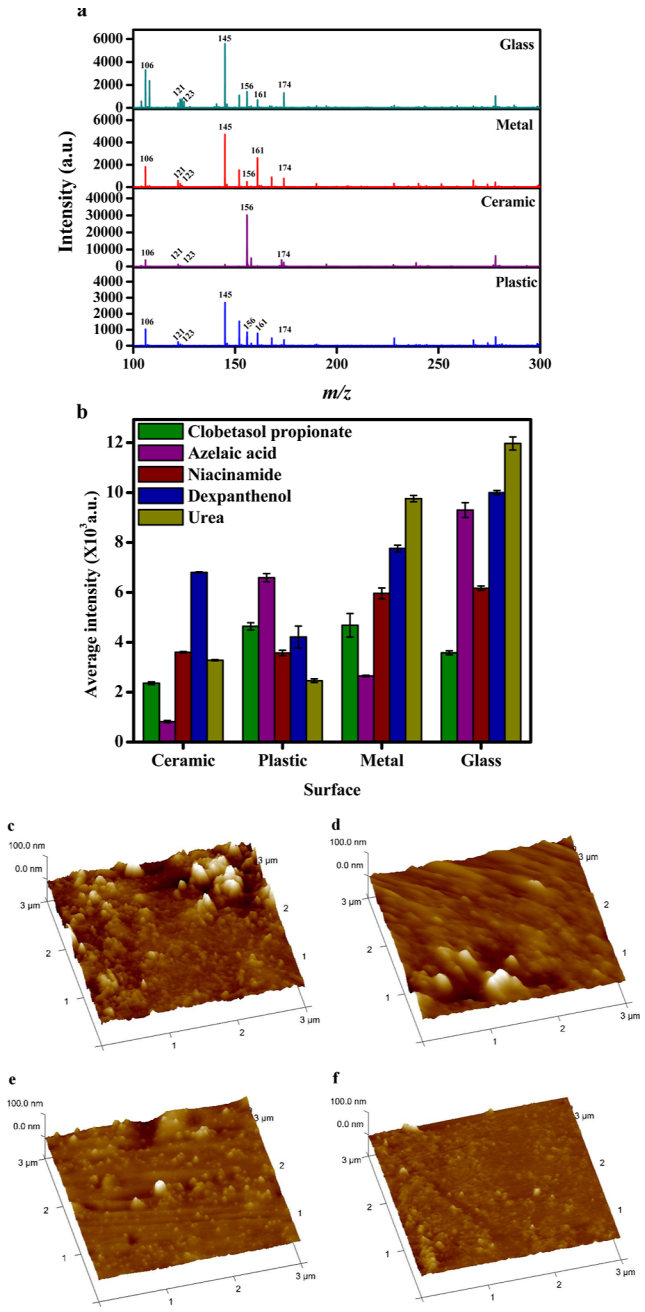

Figure 6. Analysis of FMs contaminated with cosmetic products on different surfaces. (a) Mass spectra of FMs contaminated with Ordinary serum on ceramic, plastic, metal, and glass using magnetic recovery with m/z 100−300 (as an example). (b) SALDI-MS signal intensities of APIs recovered from glass, metal, ceramic, and plastic and AFM scans in a 3 μm × 3 μm area for (c) ceramic, (d) plastic, (e) metal, and (f) glass.

valleys on the surface was observed for the ceramic and plastic surfaces, with R_a = 6.47 and 5.68 nm, respectively. In contrast, aluminum and glass in Figure 6e−f showed mountain and valley-like structures with smoother profiles. This was supported by the R_a values, which were significantly smaller than those of the ceramic and plastic, namely, R_a = 3.08 nm for aluminum and R_a = 1.81 nm for glass. Based on the AFM findings, differences in roughness could explain the lower magnetic recoveries of the contaminated FMs from the ceramic and plastic surfaces than from the aluminum and glass surfaces. Roughness can increase the hydrophobicity of a surface,[54] which can limit the movement of magnetic hydrophilic droplets and the magnetic strength, in addition to causing particle adhesion over the ceramic and plastic surfaces.

4. CONCLUSIONS

In this study, a thorough investigation into the chemical analysis, stability, and recovery of cosmetic-contaminated FM evidence was performed using mass spectrometry. A new SALDI-MS magnetic substrate was prepared, characterized, and optimized for the analysis of contaminated FMs. Initially, different ratios of CeO_2 on the surfaces of Fe_3O_4 MNPs were synthesized using a chemical coprecipitation method, and the characterization results revealed that the obtained MNPs were spherical with good UV absorbance and surface area. Subsequently, the prepared MNPs were used as SALDI-MS substrates to analyze a nicotinamide standard solution, which proved that 1:15 Fe_3O_4−CeO_2 was the optimum substrate in terms of signal intensity. Thereafter, control samples of FMs and five cosmetic products were analyzed separately to identify the major species present in FMs that were contaminated with the five cosmetic products. In both scenarios, FM components such as histidine, threonine, FA (20:1), FA (20:2), squalene, and cholesterol, as well as the APIs and other ingredients in the cosmetic products, were successfully detected. The stability of the cosmetic-contaminated FMs on the target plate varied due to the degradation behaviors of the cosmetic products' APIs; nonetheless, all APIs were detected even 28 days after deposition. Finally, magnetic recovery of cosmetics-contaminated FMs on four surfaces, namely, ceramic tile, aluminum (nonmagnetic metal), glass, and plastic, was carried out by maneuvering the magnetic substrate over the contaminated FM impressions. All APIs were detected on the hydrophobic and hydrophilic surfaces, and the recovery of each cosmetic product was greatly influenced by the texture of the cosmetic product, its composition, and the roughness of the surface. This work demonstrates the effective recovery of contaminated FM evidence for chemical analysis and its stability over time. Further development will involve functionalization of the magnetic substrate with hydrophobic and hydrophilic coatings to improve the magnetic recovery efficiency.

■ ASSOCIATED CONTENT

Supporting Information

The Supporting Information is available free of charge at https://pubs.acs.org/doi/10.1021/acsomega.2c05134.

Detailed ingredients of cosmetic products, UV−vis, and BET analysis of MNPs and SALDI-MS analysis of cosmetic products and contaminated FMs, aged FMs, and FMs recovered from different surfaces (PDF)

■ AUTHOR INFORMATION

Corresponding Author

Entesar Al-Hetlani − *Faculty of Science, Department of Chemistry, Kuwait University, Kuwait City 13060, Kuwait;* orcid.org/0000-0003-2281-6257; Email: entesar.alhetlani@ku.edu.kw

Authors

Sara A. Al-Sayed − *Faculty of Science, Department of Chemistry, Kuwait University, Kuwait City 13060, Kuwait*

https://doi.org/10.1021/acsomega.2c05134
ACS Omega 2022, 7, 43894−43903

Mohamed O. Amin − *Faculty of Science, Department of Chemistry, Kuwait University, Kuwait City 13060, Kuwait;* orcid.org/0000-0003-1305-7746

Complete contact information is available at: https://pubs.acs.org/10.1021/acsomega.2c05134

Author Contributions

CRediT authorship contribution statement: **Sara A. Al-Sayed** performed the experiments, assessed the data, and wrote the original draft. **Mohamed O. Amin** performed the experiments, conceptualized the study, and reviewed and edited the manuscript. **Entesar Al-Hetlani** administered the project, conceptualized the study, reviewed and edited the manuscript, and supervised the study.

Notes

The authors declare no competing financial interest.

■ ACKNOWLEDGMENTS

The authors gratefully acknowledge the Kuwait University Research Administration and the College of Graduate Studies (CGS) of Kuwait University. The authors thank the Department of Chemistry, Kuwait University, for performing the MALDI-TOF/TOF MS analyses.

■ REFERENCES

(1) Ricci, C.; Kazarian, S. G. Collection and detection of latent fingermarks contaminated with cosmetics on nonporous and porous surfaces. *Surf. Interface Anal.* **2010**, *42*, 386−392.
(2) Lauzon, N.; Chaurand, P. Detection of exogenous substances in latent fingermarks by silver-assisted LDI imaging MS: perspectives in forensic sciences. *Analyst* **2018**, *143*, 3586−3594.
(3) Mou, Y.; Rabalais, J. W. Detection and identification of explosive particles in fingerprints using attenuated total reflection-Fourier transform infrared spectromicroscopy. *J. Forensic Sci.* **2009**, *54*, 846−850.
(4) Amin, M. O.; Al-Hetlani, E.; Lednev, I. K. Detection and identification of drug traces in latent fingermarks using Raman spectroscopy. *Sci. Rep.* **2022**, *12*, 3136.
(5) van Helmond, W.; Kuijpers, C.-J.; van Diejen, E.; Spiering, J.; Maagdelijn, B.; de Puit, M. Amino acid profiling from fingerprints, a novel methodology using UPLC-MS. *Anal. Methods* **2017**, *9*, 5697−5702.
(6) Groeneveld, G.; de Puit, M.; Bleay, S.; Bradshaw, R.; Francese, S. Detection and mapping of illicit drugs and their metabolites in fingermarks by MALDI MS and compatibility with forensic techniques. *Sci. Rep.* **2015**, *5*, 11716.
(7) Amin, M. O.; Al-Hetlani, E.; Lednev, I. K. Trends in vibrational spectroscopy of fingermarks for forensic purposes. *TrAC, Trends Anal. Chem.* **2021**, *143*, 116341.
(8) Bleay, S. M.; Bailey, M. J.; Croxton, R. S.; Francese, S. The forensic exploitation of fingermark chemistry: A review. *WIREs Forensic Sci.* **2021**, *3*, No. e1403.
(9) Chen, H.; Shi, M.; Ma, R.; Zhang, M. Advances in fingermark age determination techniques. *Analyst* **2021**, *146*, 33−47.
(10) Chisvert, A.; Salvador, A.*Analysis of Cosmetic Products*; Elsevier, 2007.
(11) Salahioglu, F.; Went, M. J. Differentiation of lipsticks by Raman spectroscopy. *Forensic Sci. Int.* **2012**, *223*, 148−152.
(12) Raynor, I.; Coulson, S. A.; Curran, J. M.; Nair, M. V.; Miskelly, G. M.; Rindelaub, J. D. The persistence of moisturizer products on human skin in relation to sexual assault investigations. *Forensic Chem.* **2021**, *25*, 100348.
(13) López-López, M.; Vaz, J.; García-Ruiz, C. Confocal Raman spectrocopy for the analysis of nail polish evidence. *Talanta* **2015**, *138*, 155−162.
(14) Salahioglu, F.; Went, M. J.; Gibson, S. J. Application of Raman spectroscopy for the differentiation of lipstick traces. *Anal. Methods* **2013**, *5*, 5392−5401.
(15) Skobeeva, S.; Banyard, A.; Rooney, B.; Thatti, R.; Thatti, B.; Fletcher, J. Near-infrared spectroscopy combined with chemometrics to classify cosmetic foundations from a crime scene. *Sci. Justice* **2022**, *62*, 327−335.
(16) Griffin, R.; Doolan, K.; Campbell, M.; Hamill, J.; Kee, T. Analysis of wax-based products by capillary gas chromatography-mass spectrometry. *Sci. Justice* **1996**, *36*, 229−243.
(17) Pasieczna-Patkowska, S.; Olejnik, T. Analysis of cosmetic products using different IR spectroscopy techniques. *Annales UMCS Sectio AA (Chemia)* **2014**, *68*, 95.
(18) Chophi, R.; Sharma, S.; Singh, R. Discrimination of nail polish using attenuated total reflectance infrared spectroscopy and chemometrics. *Aust. J. Forensic Sci.* **2021**, *53*, 325−336.
(19) Chophi, R.; Sharma, S.; Singh, R. Forensic analysis of red lipsticks using ATR-FTIR spectroscopy and chemometrics. *Forensic Chem.* **2020**, *17*, 100209.
(20) Asri, M. N. M.; Verma, R.; Ibrahim, M. H.; Nor, N. A. M.; Sharma, V.; Ismail, D. On the discrimination between facial creams of different brands using Raman Spectroscopy and partial least squares discriminant analysis for forensic application. *Sci. Justice* **2021**, *61*, 687−696.
(21) Rowell, F.; Seviour, J.; Lim, A. Y.; Elumbaring-Salazar, C. G.; Loke, J.; Ma, J. Detection of nitro-organic and peroxide explosives in latent fingermarks by DART-and SALDI-TOF-mass spectrometry. *Forensic Sci. Int.* **2012**, *221*, 84−91.
(22) Ismail, M. M.; Amin, M. O.; Al-Hetlani, E. Analysis of drugs and pesticides for forensic purposes using noble metal-modified silica monolith as SALDI-MS substrate. *Microchem. J.* **2021**, *166*, 106201.
(23) Amin, M. O.; Al-Hetlani, E. Development of efficient SALDI substrate based on Au−TiO2 nanohybrids for environmental and forensic detection of dyes and NSAIDs. *Talanta* **2021**, *233*, 122530.
(24) Amin, M. O.; Madkour, M.; Al-Hetlani, E. Metal oxide nanoparticles for latent fingerprint visualization and analysis of small drug molecules using surface-assisted laser desorption/ionization mass spectrometry. *Anal. Bioanal. Chem.* **2018**, *410*, 4815−4827.
(25) Al-Hetlani, E.; Amin, M. O.; Madkour, M.; Nazeer, A. A. CeO2-CB nanocomposite as a novel SALDI substrate for enhancing the detection sensitivity of pharmaceutical drug molecules in beverage samples. *Talanta* **2018**, *185*, 439−445.
(26) Picca, R. A.; Calvano, C. D.; Cioffi, N.; Palmisano, F. Mechanisms of nanophase-induced desorption in LDI-MS. A short review. *Nanomaterials* **2017**, *7*, 75.
(27) AlSaeed, H.; Amin, M. O.; Al-Hetlani, E. Forensic analysis of cosmetic smudges using surface-assisted laser desorption/ionization mass spectrometry: recovery and ageing study. *Microchem. J.* **2022**, *180*, 107609.
(28) Mohammadiyan, E.; Ghafuri, H.; Kakanejadifard, A. Synthesis and characterization of a magnetic Fe3O4@ CeO2 nanocomposite decorated with Ag nanoparticle and investigation of synergistic effects of Ag on photocatalytic activity. *Optik* **2018**, *166*, 39−48.
(29) Amin, M. O.; Al-Hetlani, E.; Francese, S. Magnetic carbon nanoparticles derived from candle soot for SALDI MS analyses of drugs and heavy metals in latent fingermarks. *Microchem. J.* **2022**, *178*, 107381.
(30) Yamashita, T.; Hayes, P. Analysis of XPS spectra of Fe2+ and Fe3+ ions in oxide materials. *Appl. Surf. Sci.* **2008**, *254*, 2441−2449.
(31) Channei, D.; Inceesungvorn, B.; Wetchakun, N.; Ukritnukun, S.; Nattestad, A.; Chen, J.; Phanichphant, S. Photocatalytic degradation of methyl orange by CeO2 and Fe−doped CeO2 films under visible light irradiation. *Sci. Rep.* **2014**, *4*, 5757.
(32) Bortamuly, R.; Konwar, G.; Boruah, P. K.; Das, M. R.; Mahanta, D.; Saikia, P. CeO 2-PANI-HCl and CeO 2-PANI-PTSA composites: synthesis, characterization, and utilization as supercapacitor electrode materials. *Ionics* **2020**, *26*, 5747−5756.
(33) Lian, J.; Liu, P.; Jin, C.; Shi, Z.; Luo, X.; Liu, Q. Perylene diimide-functionalized CeO 2 nanocomposite as a peroxidase mimic

for colorimetric determination of hydrogen peroxide and glutathione. *Microchim. Acta* **2019**, *186*, 332.
(34) Madkour, M.; Allam, O. G.; Abdel Nazeer, A.; Amin, M. O.; Al-Hetlani, E. CeO2-based nanoheterostructures with p−n and n−n heterojunction arrangements for enhancing the solar-driven photodegradation of rhodamine 6G dye. *J. Mater. Sci.: Mater. Electron.* **2019**, *30*, 10857−10866.
(35) Karimzadeh, I.; Faryadi, M. Superparamagnetic Nanoparticles Doped with Copper Cations and Surface-Capped by Polyvinylpyrrolidone for Biomedical Applications. *Anal. Bioanal. Electrochem.* **2019**, *11*, 657−667.
(36) Lim, A. Y.; Ma, J.; Boey, Y. C. F. Development of Nanomaterials for SALDI-MS Analysis in Forensics. *Adv. Mater.* **2012**, *24*, 4211−4216.
(37) Nurhasanah, I.; Safitri, W.; Arifin, Z.; Subagio, A.; Windarti, T.Antioxidant activity and dose enhancement factor of CeO2 nanoparticles synthesized by precipitation method. *IOP Conference Series: Materials Science and Engineering*; IOP Publishing, 2018, *432*; p 012031.
(38) Panwar, V.; Kumar, P.; Bansal, A.; Ray, S. S.; Jain, S. L. PEGylated magnetic nanoparticles (PEG@ Fe3O4) as cost effective alternative for oxidative cyanation of tertiary amines via CH activation. *Appl. Catal., A* **2015**, *498*, 25−31.
(39) Müller, W. H.; Verdin, A.; De Pauw, E.; Malherbe, C.; Eppe, G. Surface-assisted laser desorption/ionization mass spectrometry imaging: A review. *Mass Spectrom. Rev.* **2020**, *41*, 373.
(40) Thommes, M.; Kaneko, K.; Neimark, A. V.; Olivier, J. P.; Rodriguez-Reinoso, F.; Rouquerol, J.; Sing, K. S. Physisorption of gases, with special reference to the evaluation of surface area and pore size distribution (IUPAC Technical Report). *Pure Appl. Chem.* **2015**, *87*, 1051−1069.
(41) Law, K.; Larkin, J. R. Recent advances in SALDI-MS techniques and their chemical and bioanalytical applications. *Anal. Bioanal. Chem.* **2011**, *399*, 2597−2622.
(42) Juang, Y.-M.; Chien, H.-J.; Chen, C.-J.; Lai, C.-C. Graphene flakes enhance the detection of TiO2-enriched catechins by SALDI-MS after microwave-assisted enrichment. *Talanta* **2016**, *153*, 347−352.
(43) Chaturvedi, L.; Howlader, S.; Chhikara, D.; Singh, P.; Bagga, S.; Srivatsa, K. Characteristics of nanocrystalline CeO 2 thin films deposited on different substrates at room temperature. *Indian J. Pure Appl. Phys.* **2017**, *55*, 630−637.
(44) Aziz, S. B.; Dannoun, E.; Tahir, D. A.; Hussen, S. A.; Abdulwahid, R. T.; Nofal, M. M.; Abdullah, R. M.; Hussein, A. M.; Brevik, I. Synthesis of PVA/CeO2 based nanocomposites with tuned refractive index and reduced absorption edge: Structural and optical studies. *Materials* **2021**, *14*, 1570.
(45) Saga, K. Structure and function of human sweat glands studied with histochemistry and cytochemistry. *Prog. Histochem. Cytochem.* **2002**, *37*, 323−386.
(46) Ferguson, L. S.; Creasey, S.; Wolstenholme, R.; Clench, M. R.; Francese, S. Efficiency of the dry−wet method for the MALDI-MSI analysis of latent fingermarks. *J. Mass Spectrom.* **2013**, *48*, 677−684.
(47) Lauzon, N.; Dufresne, M.; Chauhan, V.; Chaurand, P. Development of laser desorption imaging mass spectrometry methods to investigate the molecular composition of latent fingermarks. *J. Am. Soc. Mass Spectrom.* **2015**, *26*, 878−886.
(48) Emerson, B.; Gidden, J.; Lay, J. O., Jr; Durham, B. Laser desorption/ionization time-of-flight mass spectrometry of triacylglycerols and other components in fingermark samples. *J. Forensic Sci.* **2011**, *56*, 381−389.
(49) Wolstenholme, R.; Bradshaw, R.; Clench, M. R.; Francese, S. Study of latent fingermarks by matrix-assisted laser desorption/ionisation mass spectrometry imaging of endogenous lipids. *Rapid Commun. Mass Spectrom.* **2009**, *23*, 3031−3039.
(50) Sato, H.; Nakamura, S.; Fouquet, T.; Ohmura, T.; Kotani, M.; Naito, Y. Molecular characterization of polyethylene oxide based oligomers by surface-assisted laser desorption/ionization mass spectrometry using a through-hole alumina membrane as active substrate. *Rapid Commun. Mass Spectrom.* **2020**, *34*, No. e8597.
(51) Seline, K.-G.; Johein, H. The determination of l-carnitine in several food samples. *Food Chem.* **2007**, *105*, 793−804.
(52) West, M. J.; Went, M. J. The spectroscopic detection of exogenous material in fingerprints after development with powders and recovery with adhesive lifters. *Forensic Sci. Int.* **2008**, *174*, 1−5.
(53) Zhao, Y.; Xu, Z.; Parhizkar, M.; Fang, J.; Wang, X.; Lin, T. Magnetic liquid marbles, their manipulation and application in optical probing. *Microfluid. Nanofluid.* **2012**, *13*, 555−564.
(54) Zhou, Q.; Ristenpart, W. D.; Stroeve, P. Magnetically induced decrease in droplet contact angle on nanostructured surfaces. *Langmuir* **2011**, *27*, 11747−11751.

https://doi.org/10.1021/acsomega.2c05134
ACS Omega 2022, 7, 43894−43903